

SeeingSounds: Learning Audio-to-Visual Alignment via Text

Simone Carnemolla

simone.carnemolla@phd.unict.it
University of Catania
Catania, Italy

Matteo Pennisi

matteo.pennisi@unict.it
University of Catania
Catania, Italy

Chiara Russo

chiaramaria.russo@studium.unict.it
University of Catania
Catania, Italy

Simone Palazzo

simone.palazzo@unict.it
University of Catania
Catania, Italy

Daniela Giordano

daniela.giordano@unict.it
University of Catania
Catania, Italy

Concetto Spampinato

concetto.spampinato@unict.it
University of Catania
Catania, Italy

Abstract

We introduce **SeeingSounds**, a lightweight and modular framework for audio-to-image generation that leverages the interplay between audio, language, and vision—without requiring any paired audio-visual data or training on visual generative models. Rather than treating audio as a substitute for text or relying solely on audio-to-text mappings, our method performs dual alignment: audio is projected into a semantic language space via a frozen language encoder, and contextually grounded into the visual domain using a vision-language model. This approach, inspired by cognitive neuroscience, reflects the natural cross-modal associations observed in human perception. The model operates on frozen diffusion backbones and trains only lightweight adapters, enabling efficient and scalable learning. Moreover, it supports fine-grained and interpretable control through procedural text prompt generation, where audio transformations (e.g., volume or pitch shifts) translate into descriptive prompts (e.g., “a distant thunder”) that guide visual outputs. Extensive experiments across standard benchmarks confirm that SeeingSounds outperforms existing methods in both zero-shot and supervised settings, establishing a new state of the art in controllable audio-to-visual generation.

CCS Concepts

• **Computing methodologies** → *Image representations*; **Image representations**.

Keywords

Multimodal Generation, Audio to Image

ACM Reference Format:

Simone Carnemolla, Matteo Pennisi, Chiara Russo, Simone Palazzo, Daniela Giordano, and Concetto Spampinato. 2025. SeeingSounds: Learning Audio-to-Visual Alignment via Text. In *ACM Multimedia Asia (MMAsia '25)*, December 9–12, 2025, Kuala Lumpur, Malaysia. ACM, New York, NY, USA, 7 pages. <https://doi.org/10.1145/3743093.3770976>

1 Introduction

Generative models conditioned on textual descriptions have led to remarkable progress in image and video synthesis. Models like DALL-E [27] and Stable Diffusion [29] have demonstrated that large-scale training on vision-language data enables highly expressive and coherent generation. Beyond text conditioning, recent works have explored audio as a complementary modality for visual synthesis, motivated by its natural co-occurrence with visual events and its ability to convey contextual and temporal information.

Early approaches to audio-conditioned image synthesis primarily relied on Generative Adversarial Networks (GANs) [8, 9, 14, 18, 19, 33], showing that sound can guide visual generation but often operating on constrained datasets with strong audio-visual correlations, and focusing more on style manipulation than true synthesis. To improve generation quality and scalability, recent works have increasingly adopted diffusion models, leveraging powerful pre-trained text-to-image architectures while introducing audio-to-text mappings to recycle existing language supervision [11, 24, 37]. While these approaches are effective, they typically treat language as the sole intermediary—aligning audio to vision indirectly through text. SonicDiffusion [17] takes a step further by injecting audio features directly into the diffusion process via cross-attention, resulting in high-quality audio-guided generation. However, these methods overlook the deeper, complementary relationships between *language, hearing, and vision* - interconnections that are strongly supported by cognitive neuroscience as foundational to human perception [2, 10, 30].

This evolving line of research coincides with a broader shift in generative modeling: diffusion models now support richer conditioning interfaces, enabled by dedicated encoders for multiple input types. Recent multimodal frameworks like Flux [15] have extended this paradigm, employing modular adapters and mapping networks to integrate information from diverse sources such as audio, language, and vision.

Building on this recent shift toward multimodal conditioning in generative modeling, we propose **SeeingSounds**, a lightweight and modular framework for controllable visual generation via *tri-modal alignment* between audio, language, and vision. Our approach leverages multi-encoder diffusion architectures and introduces two core text-mediated alignment paths: (i) an *audio-to-text* mapping through a frozen language model, and (ii) a *text-to-vision* grounding via CLIP. This design enables our model to generate images directly from audio, without relying on paired audio-visual

arXiv:2510.11738v1 [cs.LG] 10 Oct 2025



This work is licensed under a Creative Commons Attribution 4.0 International License. *MMAsia '25, Kuala Lumpur, Malaysia*
© 2025 Copyright held by the owner/author(s).
ACM ISBN 979-8-4007-2005-5/2025/12
<https://doi.org/10.1145/3743093.3770976>

data during training. Crucially, conversely to existing diffusion-based approaches, we do not train or fine-tune the diffusion model, only lightweight adapters on top of frozen backbones are optimized.

A key strength of our framework is its controllability, enabled by the intermediate text-based alignment. Audio modifications are translated into textual prompts—e.g., lowering the volume of a train sound yields “*the sound of a distant train*”—which guide generation in a semantically consistent and interpretable way. This allows for fine-grained control without modifying or fine-tuning the generative model.

We evaluate it across a wide set of benchmarks — VEGAS [39], VGGSound [7], Landscape [16] combined to Into the Wild [19] and RAVDESS [20] — spanning diverse acoustic environments, material interactions, natural scenes, and emotional expressions. Our results show state-of-the-art performance in audio-to-scene generation, both qualitatively and quantitatively, confirming the effectiveness of our simple yet effective *language-vision-audio* alignment strategy. To summarize, the contributions of this work are:

- A lightweight and modular framework for visual generation from audio, trained without the need for any paired audio-visual data.
- An alignment strategy that bridges audio, language, and vision through semantically grounded connections.
- An interpretable and controllable generation pipeline that allows procedural audio modifications to be reflected in the visual output via text-mediated prompt manipulation;
- A thorough empirical evaluation demonstrating strong generalization and significantly outperforming prior methods on zero-shot audio-to-image benchmarks.

2 Related work

Audio-driven visual synthesis spans image and video generation. Early work mainly used VAEs/GANs to bridge audio–image semantics [8, 9, 14, 18, 19, 22, 33]. Notably, SGSIM [18] and Sound2Scene [31] injected CLIP/ResNet audio embeddings into pretrained GANs (e.g., StyleGAN/BigGAN) with contrastive losses, but struggled on in-the-wild data, with low semantic fidelity and weak generalization. Robust-SGSIM [17] added KL-regularization between audio–image and text–image cosine-similarity distributions, among the first to combine audio–text–image. AVStyle [19] used audiovisual adversarial training and patch-wise contrastive learning for stylization. Despite these advances, diffusion models have surpassed GANs in quality, fidelity, and scalability. Diffusion-era methods condition generation on audio via learned multimodal spaces. GlueGen [24] fuses XLM-R (text) and AudioCLIP [13] features, aligned in CLIP space for latent diffusion. AudioToken [37] injects audio directly into CLIP’s text-token space. These rely on indirect audio–image alignment. ImageBind [11] learns a joint space for audio–image–text (and more) via InfoNCE, but targets retrieval/representation rather than controllable generation. SonicDiffusion [3] adapts Stable Diffusion with audio-aware cross-attention for high-quality audio-guided synthesis/editing, yet mediates audio through text, without explicit trimodal alignment.

We introduce a lightweight trimodal framework that semantically aligns audio, language, and vision. Using frozen encoders with

small adapters trained on disjoint audio–text and text–image corpora, we avoid any paired audio–visual data. Our approach offers fine-grained, interpretable control via procedural prompt manipulation: audio changes (e.g., pitch/volume) map to textual prompts (e.g., “a distant thunder”) that steer generation—without tuning the generative model.

3 Method

We propose an alignment framework for audio-conditioned visual generation that leverages language as an intermediary to connect the auditory and visual domains. Central to our approach is our alignment strategy: one branch of the architecture aligns audio features to textual semantics, while the other aligns audio features to a vision-aware latent space via language. This enables the model to benefit from the compositional structure of natural language and the grounding power of large-scale vision-language models, without requiring the need of visual data at training time. Furthermore, unlike existing and recent methodologies [3, 38], our pure alignment-based design does not involve the visual generation model in any way, allowing for a more efficient training paradigm.

Let $\mathcal{D} = \{(\mathbf{a}_1, y_1), (\mathbf{a}_2, y_2), \dots, (\mathbf{a}_n, y_n)\}$ be an audio dataset, where each audio sample \mathbf{a}_i is associated with a class label $y_i \in \mathcal{C}$, $|\mathcal{C}| = k$. For each class in \mathcal{C} , we also assume the availability of a corresponding textual description, building up a set $\mathcal{T} = \{t_1, t_2, \dots, t_k\}$ of “class-level captions”. This requirement aligns with similar approaches in the literature [3], which utilize image data with image-level captions obtained via pre-trained captioning models. Our approach relaxes this requirement by needing only a class-level caption for each class obtained by prompting a large language model (system prompts are reported in supplementary materials).

Given an audio sample (\mathbf{a}, y) , we employ a transformer-based audio encoder E_A as a feature extractor, to derive a latent representation \mathbf{f} in the form of a sequence of tokens:

$$\mathbf{f} = E_A(\mathbf{a}) = [\mathbf{f}_1, \mathbf{f}_2, \dots, \mathbf{f}_m], \quad (1)$$

where each $\mathbf{f}_i \in \mathbb{R}^{d_A}$ and d_A is the dimensionality of each audio token. Our goal is to align this audio representation with the representations generated by a text encoder E_T and a vision-language encoder E_V , both conditioned by the class captions in \mathcal{T} .

The text encoder E_T is a pure textual model that, given sample (\mathbf{a}, y) , processes a tokenized version of the class-level caption t_y , transforming it into a sequence of output tokens $\mathbf{z}_T = E_T(t_y) = [\mathbf{z}_{T,1}, \mathbf{z}_{T,2}, \dots, \mathbf{z}_{T,l}]$, with each $\mathbf{z}_{T,i} \in \mathbb{R}^{d_T}$, where d_T is the dimensionality of the textual representation. In contrast, the vision-language encoder E_V , while being similarly conditioned by the caption t_y , is designed to produce a vision-aware representation of the input text, as done by CLIP [25] and similar models. The output of the vision-language encoder E_V is a vector $\mathbf{z}_V = E_V(t_y) \in \mathbb{R}^{d_V}$, with d_V being the dimensionality of the embedding space.

To facilitate the alignment of audio features \mathbf{f} with \mathbf{z}_T and \mathbf{z}_V , we introduce adapter modules A_T and A_V to project audio feature tokens onto the same dimensionality as the target representations. Each module is implemented as a multi-layer perceptron, producing the corresponding adapted features \mathbf{w}_T and \mathbf{w}_V :

$$\mathbf{w}_T = A_T(\mathbf{f}) = [\mathbf{w}_{T,1}, \mathbf{w}_{T,2}, \dots, \mathbf{w}_{T,m}], \quad (2)$$

$$\mathbf{w}_V = A_V(\mathbf{f}) = [\mathbf{w}_{V,1}, \mathbf{w}_{V,2}, \dots, \mathbf{w}_{V,m}], \quad (3)$$

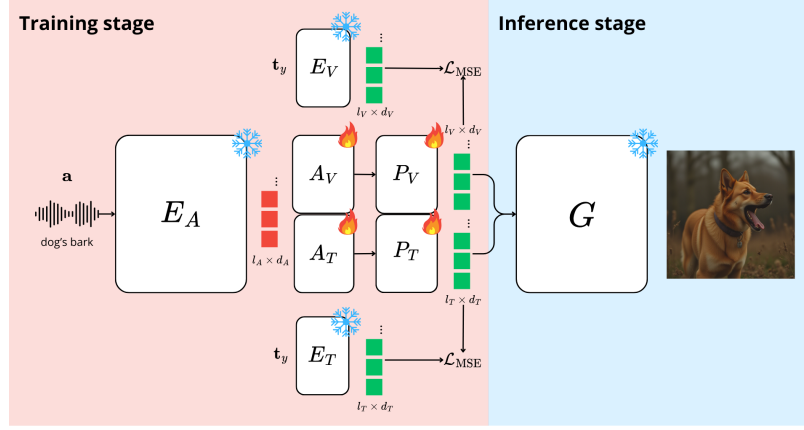


Figure 1: Overview of audio-text and visual modal alignment in Seeing Sounds. During training (left), audio features E_A are aligned to both language and vision-language spaces via lightweight adapters (A_T and A_V) and projected (through P_T and P_V) using MSE losses against frozen text (E_T) and vision-text (E_V) encoders. At inference (right), the audio-text-vision-aligned projection conditions a frozen diffusion model for audio-driven image generation, enabling controllable and paired-free synthesis.

with $w_{T,i} \in \mathbb{R}^{d_T}$ and $w_{V,i} \in \mathbb{R}^{d_V}$.

The final step before feature alignment consists in matching the lengths of the sequences in w_T and w_V with those of, respectively, z_T and z_V . Indeed, w_T and w_V come directly from the encoded input sequence \mathbf{f} , which contains m tokens; instead, the number of tokens in z_T depends on the caption \mathbf{t}_y (which has l tokens), while z_V is a single vector. To solve this discrepancy, we employ attention pooling [6], which allows for a flexible mapping between the different lengths of the sequences. Attention pooling projects a sequence of p tokens to q tokens, utilizing q learnable query tokens and performing self-attention over the entire set of tokens to learn the mapping from the original p tokens. This method is preferred over alternative pooling strategies (e.g., token averaging or concatenation) due to its ability to capture complex relationships between tokens, as well as its natural application to token-structured data.

Let $P_{p,q,\theta}$ denote the attention pooling operation, which transforms a sequence of p tokens into q tokens using parameters θ . The pooled representations are computed as follows:

$$\hat{z}_T = P_{m,l,\theta_T}(\mathbf{w}_T) = P_T(\mathbf{w}_T) = [\hat{z}_{T,1}, \dots, \hat{z}_{T,l}], \quad (4)$$

$$\hat{z}_V = P_{m,1,\theta_V}(\mathbf{w}_V) = P_V(\mathbf{w}_V) \in \mathbb{R}^{d_V}, \quad (5)$$

where θ_T and θ_V are the parameters of the two pooling layers (i.e., the learned query tokens and the cross-attention projection matrices), and each $\hat{z}_{T,j} \in \mathbb{R}^{d_T}$.

The resulting representations \hat{z}_T and \hat{z}_V are subsequently fed into a visual generator G to produce the output image $\mathbf{v} = G(\hat{z}_T, \hat{z}_V)$.

During the training phase, we optimize the parameters of the adapter modules and attention pooling layers, while keeping the encoders E_A , E_T , E_V , and the generator G frozen. Let $\hat{z}_T(\cdot)$ and $\hat{z}_V(\cdot)$ denote the process of computing \hat{z}_T and \hat{z}_V from \mathbf{a} ; similarly, let $z_T(\cdot)$ and $z_V(\cdot)$ compute the target representations z_T and z_V from \mathbf{y} (and hence \mathbf{t}_y). The alignment of the learned representations is achieved by minimizing the mean square error (MSE) loss between

the generated and target representations:

$$\begin{aligned} \mathcal{L}_{\text{MSE}} &= \frac{1}{n} \sum_{(\mathbf{a}, \mathbf{y})} [\|\hat{z}_T(\mathbf{a}) - z_T(\mathbf{t}_y)\|^2 + \|\hat{z}_V(\mathbf{a}) - z_V(\mathbf{t}_y)\|^2] \\ &= \frac{1}{n} \sum_{(\mathbf{a}, \mathbf{y})} \mathcal{L}(\mathbf{a}, \mathbf{t}_y), \end{aligned} \quad (6)$$

with \mathcal{L} representing, for brevity, the loss contribution of a single sample.

This training strategy enables an effective and efficient model training process, maintaining a limited number of learnable parameters and circumventing the need for backpropagation through the diffusion model, which is typically computationally intensive.

3.1 Enhancing controllability

Since the generation process is mediated by textual semantics, without any requirement for training images, we can guide the audio-to-visual generation process by manipulating the input audio signal and the associated class-level captions. This allows us to effectively generate additional “pseudo-classes”, extending the range of audio variability that our model can render into visual scenes. For instance, consider an audio recording of a train: the associated class caption might be “a train is passing by”. By modifying the audio signal — e.g., attenuating the volume or adding reverberation — we can correspondingly change the descriptive text to “a distant train” or “a train echoing in a tunnel”. Importantly, this whole procedure can be carried out programmatically, by predefining the set of augmentation effects, and computing the associated captions through a large language model (LLM). An added benefit of this procedure is that it also enables the capability of modeling *mixed* audio signals by combining the respective descriptions, unlike other approaches that require non-trivial and unrealistic image-level superimposition.

Formally, let (\mathbf{a}, \mathbf{y}) be a sample from the audio dataset, and \mathbf{t}_y the corresponding class-level caption. Let $\{(T_1, \mathbf{d}_1), \dots, (T_h, \mathbf{d}_h)\}$ be a set of audio transformations: to each transformation function T_j , a

textual *transformation description* \mathbf{d}_j is associated, which describes the effect of applying T_j to an audio sample \mathbf{a} . Then, let f be a text transformation function that, given a class-level caption \mathbf{t}_y and a transformation description \mathbf{d}_j , stochastically produces an updated version of \mathbf{t}_y , in light of applying the transformation described by \mathbf{d}_j .

Additionally, let (\mathbf{a}_i, u) and (\mathbf{a}_j, v) be two samples from the dataset, and g be another text transformation function, which acts on the class-level captions \mathbf{t}_u and \mathbf{t}_v to produce a description \mathbf{t}_{u+v} of a scene featuring the concepts described by the captions: our assumption is that \mathbf{t}_{u+v} is a plausible description of the audio signal obtained as $\mathbf{a}_i + \mathbf{a}_j$.

The generated semantically-consistent pairs – procedurally modified audio and edited captions – are used to supervise the training process, encouraging the model to capture nuanced audio-text relationships. The alignment objective in Eq. 6 is updated to include this extended set:

$$\begin{aligned} \mathcal{L}_{\text{ext}} = & \frac{1}{n} \sum_{(\mathbf{a}, y)} \mathcal{L}(\mathbf{a}, \mathbf{t}_y) + \\ & + \frac{1}{nh} \sum_{(\mathbf{a}, y)} \sum_{j=1}^h \mathcal{L}(T_j(\mathbf{a}), f(\mathbf{t}_y, \mathbf{d}_j)) + \\ & + \frac{1}{n(n-1)} \sum_{\substack{(\mathbf{a}_i, u), \\ (\mathbf{a}_j, v)}} \mathcal{L}(\mathbf{a}_i + \mathbf{a}_j, g(\mathbf{t}_u, \mathbf{t}_v)). \end{aligned} \quad (7)$$

In practice, we manually provide the transformation descriptions, while f and g are implemented by prompt-engineering an LLM. Details are provided in the supplementary materials.

This formulation enables the model to learn a disentangled representation space, where variations in the audio domain are reflected in semantically meaningful changes in the generated visuals, improving generalization capabilities even with synthetic supervision.

4 Experimental Results

4.1 Training/evaluation setup

We use AST [12], pretrained on AudioSet, as audio encoder and Flux diffusion [15] with a pretrained LoRA adapter for image generation. Text prompts are embedded via CLIP [25] and T5 [26]. During training, image generation is disabled to speed up convergence, and model selection is based on validation loss. Prompts for each dataset class are generated with GPT-4o, using standardized system prompts (details in supplementary), and follow best practices in prompt engineering [1, 4, 28, 34, 35]. Due to different encoder dynamics, we use separate AdamW optimizers: T5 parameters use a 1×10^{-5} learning rate; CLIP-aligned ones use 1×10^{-7} . All experiments run on a single NVIDIA H100 GPU. We strictly follow training and evaluation protocols from prior work and use reported competitor results.

For VGGSound [7] and VEGAS [39], we adopt the Sound2Scene protocol [31], using the 50-class VGGSound subset with a 90/10 validation split, and both full and 5-class versions of VEGAS (800/50 samples per class for train/test). For RAVDESS [20] and Into the Wild + Landscape [16, 19], we apply the training procedures in [3], using 90/10 splits. Early stopping is applied across all benchmarks. We also test zero-shot performance on ESC-50 [23], generating

one image per sample (2,000 total) without training. Competitors are evaluated using their published results, except: 1) AudioToken was retrained on VGGSound-50 for comparability with [31]; 2) ImageBind was evaluated using its pretrained weights and Stable Diffusion UnCLIP, as in [3, 38]. For ESC-50, we retain Sound2Scene and AudioToken original weights. Inference uses mixed-precision for efficiency. We fix diffusion steps to 10, with 3.10s average generation time per image.

While [3] include the Greatest Hits dataset [21], we exclude it from quantitative evaluation due to insufficient protocol details, providing only qualitative results for illustration in the supplementary.

For controllability tests, we scale input audio using a gain factor $\alpha \in [0.1, 0.5]$, with corresponding labels: “low-volume” ($\alpha < 0.2$), “medium-volume” ($0.2 < \alpha < 0.5$), and “high-volume” (otherwise). In mixed controllability, input audio combines samples from two classes, and the caption reflects both, enabling evaluation on ambiguous content.

Additional dataset and metric details can be found in the supplementary and at the following link: [SeeingSounds supplementary](#).

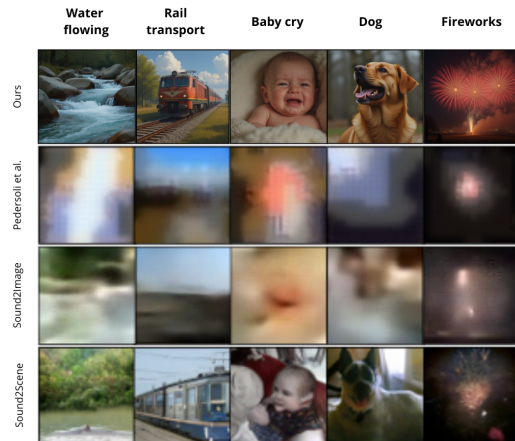


Figure 2: Qualitative results on VEGAS (5-class subset). Our model yields semantically accurate generations aligned with the input audio category. Images adapted from [31] to include our results.

4.2 Results

Comparison to state of the art methods. We start our evaluation by comparing the performance of our method with several state-of-the-art methods, including GAN-based techniques (e.g., SGSIM [18], Sound2Scene [31]), embedding-based methods (e.g., AudioToken [38], ImageBind [11]), and recent diffusion-based approaches (e.g., GlueGen [24], SonicDiffusion [3], TempoTokens [36], CoDi [32]). Evaluation is conducted using two key metrics: AIC (Audio-Image Content) and AIS (Audio-Image Similarity), where higher scores indicate stronger audio-visual alignment. As mentioned in Section 4.1, we rely exclusively on results reported in the original publications of each method. Consequently, not all baselines are evaluated on every dataset due to differences in experimental setups, training requirements, or dataset compatibility

Table 1: Comparison with state-of-the-art models on VGGSound and VEGAS. We report AIC and Recall@5 (R@5) on the 50-class subset of VGGSound and the full and 5-class VEGAS datasets respectively.

	VGGSound		VEGAS		VEGAS5
	AIC	R@5	AIC	R@5	AIC
Pedersoli et al. [22]	-	-	-	-	23.10
S2I [9]	-	-	-	-	39.19
ICGAN [5]	30.06	62.59	46.60	82.48	-
Sound2Scene [31]	40.71	77.36	57.44	84.08	77.58
ImageBind [11]	40.62	74.72	-	-	-
AudioToken [38]	41.30	77.42	-	-	-
Ours	66.64	91.60	90.81	96.28	94.30

Table 2: Cross-dataset comparison on RAVDESS, Landscape + Into the Wild, and Greatest Hits. Our model achieves the highest AIC across all benchmarks, despite using no paired audio-visual training data or diffusion model fine-tuning.

	RAVDESS		Into the wild + Landscape	
	AIS	AIC	AIS	AIC
SGSIM [18]	50.53	12.57	72.24	21.66
Sound2Scene [31]	50.90	11.08	74.66	36.72
GlueGen [24]	50.52	22.52	66.32	46.18
ImageBind [11]	58.02	21.31	72.09	46.18
CoDi [32]	52.92	13.96	75.78	46.00
AudioToken [38]	50.09	18.21	69.83	36.18
SonicDiffusion [3]	53.09	23.16	74.46	28.51
TempoTokens [36]	-	-	73.90	54.36
Ours	51.41	35.39	76.16	79.13

across methods. Table 1 reports performance on the VGGSound (50-class subset) and the VEGAS dataset, including its smaller 5-class version proposed in [31]. Our model achieves a substantial improvement over all baselines, with about 25 AIC and 14 R@5 gain over the best previous methods on VGGSound, and a large margin of AIC and R@5 gain also on both versions of VEGAS. Table 2 presents a broader comparison on RAVDESS and Landscape + Into the Wild. Our method consistently outperforms prior approaches, achieving the highest AIC scores on both RAVDESS (35.39) and Landscape + Into the Wild (79.13), with substantial margins over baselines such as SonicDiffusion and GlueGen. While our AIS score is lower than ImageBind’s one, it is worth noting that ImageBind is a foundation model specifically trained on large-scale multimodal data to perform cross-modal alignment. In contrast, our method achieves stronger semantic fidelity—as reflected in AIC—using lightweight alignment modules and without any end-to-end training of the diffusion model.

As shown in Tables 1 and 2, our model achieves consistent and substantial improvements across all datasets through a lightweight training pipeline that does not rely on visual inputs or paired audio-visual data. These results cumulatively demonstrate the power and flexibility of our trimodal alignment strategy, which enables

Table 3: Zero-shot evaluation on the ESC-50 dataset. Our model achieves significantly higher AIC and Recall@5 scores than prior works, demonstrating superior generalization to unseen audio domains.

	ESC50	
	AIC	R@5
Sound2Scene [31]	4.10	16.40
AudioToken [38]	9.00	22.00
Ours	22.60	41.35

visually coherent and semantically grounded generation from sound without training large generative backbones.

We further assess the effectiveness of our approach through qualitative comparisons. Figure 2 shows generations from the VEGAS 5-class subset, where our method produces visually coherent and semantically appropriate scenes across diverse sound categories, outperforming previous methods in clarity, object fidelity, and spatial composition. While part of this improvement may stem from leveraging a diffusion-based architecture over less expressive GANs, supplementaries extend the comparison to more challenging datasets—including RAVDESS, Landscape + Into the Wild, and Greatest Hits—where we benchmark against recent diffusion-based methods such as SonicDiffusion, AudioToken, and GlueGen. Our model consistently produces high-quality, context-aware visuals that reflect subtle audio cues, such as emotional intonation or material properties. These visual comparisons highlight the expressive capacity and generalization ability of our controllable, audio-conditioned generation pipeline.

Zero-shot performance. To evaluate the generalization capacity of our method beyond the training distribution, we conduct a zero-shot image generation experiment on the ESC-50 dataset, which comprises environmental sound clips from diverse categories such as animal calls, machinery, weather, and human vocalizations. Crucially, this dataset is never seen during training, making it ideal for testing out-of-distribution performance. We compare our approach against existing methods that release pretrained weights suitable for inference-time use, ensuring a fair and reproducible comparison without retraining. This constraint limits the pool of competitors but avoids discrepancies caused by inconsistent training pipelines. As shown in Table 3, our method achieves a substantial improvement over prior work—more than doubling the AIC and R@5 scores of the strongest baseline (AudioToken [38]).

Controllability. To assess the effectiveness of our controllable generation mechanism described in Sect. 3.1, we qualitatively explore how structured manipulations in the audio domain—either through signal transformations or compositional mixing—result in corresponding and semantically aligned changes in the generated visual output. Fig. 3 shows the controllability of our model with respect to audio intensity. Specifically, we apply a simple volume attenuation to an audio recording (e.g., of a train or a helicopter) and modify its associated text prompt accordingly (e.g., from “a train is passing” to “a distant train”). As illustrated in the generated samples, our method is capable of reflecting such subtle, continuous auditory variations into the visual modality, producing semantically faithful differences in scale, perspective, or contextual framing. For instance,

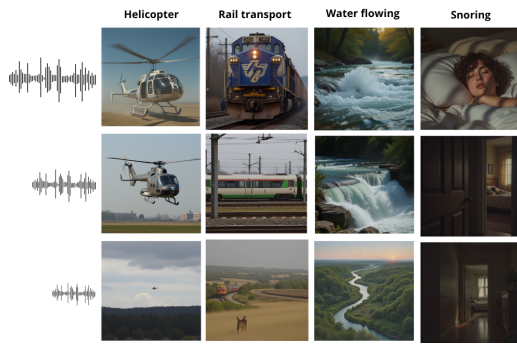


Figure 3: Volume controllability: controllable generation based on audio intensity. Lower volume yields smaller or distant visual representations.

quieter inputs often yield smaller or more distant visual objects, consistent with human perceptual expectations. In Figure 4, we demonstrate the model’s ability to synthesize scenes from *compositional audio inputs*. Each cell in the grid corresponds to a generated image conditioned on the mix of two distinct audio sources (e.g., “train” and “helicopter”) and a compositional prompt automatically derived via LLM-assisted caption fusion (e.g., “a distant train and a hovering helicopter”). The model exhibits the capacity to visually represent both acoustic sources in a coherent scene, often arranging them spatially or contextually in a way that matches the semantic structure of the textual prompt. This compositional controllability is particularly challenging for conventional approaches, which often require unrealistic pixel-level superimpositions or explicit supervision.



Figure 4: Mixed-class controllability. Each cell visualizes a scene combining the row and column audio classes (e.g. helicopter flying + rail transport).

Ablation. We finally perform a focused ablation study on the 5-class VEGAS subset to validate our architectural choices. As shown in Table 4, we first examine the role of the attention pooling modules by replacing them with simpler alternatives: adaptive pooling for the T5 branch and mean pooling for the CLIP branch of FLUX.

Table 4: Ablation study on the VEGAS 5-class subset. We assess the impact of removing attention pooling and isolating each alignment branch. Results confirm the benefit of both attention mechanisms and the full tri-modal alignment.

Model Variant	AIC
w/o attention pooling (adaptive + mean)	54.72
Only CLIP alignment	51.10
Only T5 alignment	91.00
Ours (full: T5 + CLIP + attn pooling)	94.30

This leads to a notable drop in AIC, confirming that our cross-modal attention pooling layers play a critical role in semantic alignment. When isolating each alignment branch, we observe that using only T5-based alignment outperforms the CLIP-only variant, indicating that language supervision provides stronger semantic grounding when used alone. Nonetheless, the full model—combining both alignments with attention pooling—achieves the best performance, demonstrating the complementary nature of linguistic and visual semantics in guiding audio-to-visual generation. Supplementary materials report a first extension on video-generation, multiple audio-image and audio-video samples including qualitatively results on all the employed benchmarks.

5 Conclusion

In this work, we introduced **SeeingSounds**, a lightweight and scalable framework for audio-conditioned image generation that unifies audio, language, and vision through a tri-modal alignment strategy. Departing from prior methods that rely on paired audio-visual data or require training large generative backbones, our approach leverages frozen pre-trained encoders with minimal trainable components to align audio to text via a semantic language model and text to vision through CLIP. This indirect yet effective grounding strategy eliminates the need for costly paired data and supports zero-shot generation. Extensive evaluations across multiple benchmarks demonstrate that our method consistently outperforms existing approaches, particularly in challenging low-resource or disjoint-modality settings, while maintaining strong semantic fidelity and generalization. Moreover, the introduction of procedurally generated captions tied to audio augmentations enables fine-grained controllability over the generation process. Our model can respond meaningfully to subtle changes in the input sound or composite multiple audio sources into coherent visual scenes.

Overall, SeeingSounds underscores the effectiveness of language as a bridge for multimodal grounding and open new directions for scalable, controllable, and cognitively inspired generative models.

Acknowledgments

Simone Carnemolla, Matteo Pennisi, Simone Palazzo, Daniela Giordano, and Concetto Spampinato have been supported by the European Union – Next Generation EU, Mission 4 Component 2 Line 1.3, through the PNRR MUR project PE0000013 – FAIR “Future Artificial Intelligence Research” (CUP E63C22001940006).

References

- [1] Xavier Amatriain. 2024. Prompt design and engineering: Introduction and advanced methods. *arXiv preprint arXiv:2401.14423* (2024).
- [2] Sarah H. Baum, Randi C. Martin, A. Cris Hamilton, and Michael S. Beauchamp. 2012. Multisensory speech perception without the left superior temporal sulcus. *NeuroImage* 62, 3 (2012), 1825–1832. doi:10.1016/j.neuroimage.2012.05.034
- [3] Burak Can Biner, Farrin Marouf Sofian, Umur Berkay Karakaş, Duygu Ceylan, Erkut Erdem, and Aykut Erdem. 2024. SonicDiffusion: Audio-Driven Image Generation and Editing with Pretrained Diffusion Models. arXiv:2405.00878 [cs.CV]
- [4] Tom Brown, Benjamin Mann, Nick Ryder, Melanie Subbiah, Jared D Kaplan, Prafulla Dhariwal, Arvind Neelakantan, Pranav Shyam, Girish Sastry, Amanda Askell, et al. 2020. Language models are few-shot learners. *Advances in neural information processing systems* 33 (2020), 1877–1901.
- [5] Arantxa Casanova, Marlène Careil, Jakob Verbeek, Michal Drozdal, and Adriana Romero. 2021. Instance-Conditioned GAN. *arXiv preprint arXiv:2109.05070* (2021). <https://arxiv.org/abs/2109.05070>
- [6] Fang Chen, Gourav Datta, Souvik Kundu, and Peter A Beerel. 2023. Self-attentive pooling for efficient deep learning. In *Proceedings of the IEEE/CVF Winter Conference on Applications of Computer Vision*. 3974–3983.
- [7] Honglie Chen, Weidi Xie, Andrea Vedaldi, and Andrew Zisserman. 2020. Vg-sound: A large-scale audio-visual dataset. In *ICASSP 2020-2020 IEEE International Conference on Acoustics, Speech and Signal Processing (ICASSP)*. IEEE, 721–725.
- [8] Lele Chen, Sudhanshu Srivastava, Zhiyao Duan, and Chenliang Xu. 2017. Deep cross-modal audio-visual generation. In *Proceedings of the on Thematic Workshops of ACM Multimedia*.
- [9] Leonardo A. Fanzeres and Climent Nadeu. 2021. Sound-to-imagination: Unsupervised crossmodal translation using deep dense network architecture. In *arXiv preprint arXiv:2106.01266*.
- [10] Asif A. Ghazanfar and Charles E. Schroeder. 2006. Is neocortex essentially multisensory? *Trends in Cognitive Sciences* 10, 6 (2006), 278–285. doi:10.1016/j.tics.2006.04.008
- [11] Rohit Girdhar, Alaeldin El-Nouby, Zhuang Liu, Mannat Singh, Kalyan Vasudev Alwala, Armand Joulin, and Ishan Misra. 2023. Imagebind: One embedding space to bind them all. In *Proceedings of the IEEE/CVF conference on computer vision and pattern recognition*. 15180–15190.
- [12] Yuan Gong, Yu-An Chung, and James Glass. 2021. AST: Audio Spectrogram Transformer. In *Proc. Interspeech 2021*. 571–575.
- [13] Andrey Guzhov, Federico Raue, Jörn Hees, and Andreas Dengel. 2022. Audioclip: Extending Clip to Image, Text and Audio. In *ICASSP 2022 - 2022 IEEE International Conference on Acoustics, Speech and Signal Processing (ICASSP)*. 976–980. doi:10.1109/ICASSP43922.2022.9747631
- [14] Wangli Hao, Zhaoxiang Zhang, and He Guan. 2018. CMC-GAN: A uniform framework for cross-modal visual-audio mutual generation. In *AAAI Conference on Artificial Intelligence*.
- [15] Black Forest Labs. 2024. FLUX. <https://github.com/black-forest-labs/flux>.
- [16] Seung Hyun Lee, Gyeongrok Oh, Wonmin Byeon, Chanyoung Kim, Won Jeong Ryoo, Sang Ho Yoon, Hyunjun Cho, Jihyun Bae, Jinkyu Kim, and Sangpil Kim. 2022. Sound-Guided Semantic Video Generation. In *Computer Vision – ECCV 2022*, Shai Avidan, Gabriel Brostow, Moustapha Cissé, Giovanni Maria Farinella, and Tal Hassner (Eds.). Springer Nature Switzerland, Cham, 34–50.
- [17] Seung Hyun Lee, Gyeongrok Oh, Wonmin Byeon, Sang Ho Yoon, Jinkyu Kim, and Sangpil Kim. 2023. Robust Sound-Guided Image Manipulation. In *arXiv preprint arXiv:2208.14114*.
- [18] Seung Hyun Lee, Wonseok Roh, Wonmin Byeon, Sang Ho Yoon, Chanyoung Kim, Jinkyu Kim, and Sangpil Kim. 2022. Sound-guided semantic image manipulation. In *IEEE Conference on Computer Vision and Pattern Recognition (CVPR)*.
- [19] Tingle Li, Yichen Liu, Andrew Owens, and Hang Zhao. 2022. Learning Visual Styles from Audio-Visual Associations. In *Computer Vision – ECCV 2022*, Shai Avidan, Gabriel Brostow, Moustapha Cissé, Giovanni Maria Farinella, and Tal Hassner (Eds.). Springer Nature Switzerland, Cham, 235–252.
- [20] Steven R. Livingstone and Frank A. Russo. 2018. The Ryerson Audio-Visual Database of Emotional Speech and Song (RAVDESS): A dynamic, multimodal set of facial and vocal expressions in North American English. *PLOS ONE* 13, 5 (05 2018), 1–35. doi:10.1371/journal.pone.0196391
- [21] Andrew Owens, Phillip Isola, Josh McDermott, Antonio Torralba, Edward H. Adelson, and William T. Freeman. 2016. Visually Indicated Sounds. In *Proceedings of the IEEE Conference on Computer Vision and Pattern Recognition (CVPR)*.
- [22] Fabrizio Pedersoli, Dryden Wiebe, Amin Banitalebi, Yong Zhang, George Tzantakakis, and Kwang M. Yi. 2022. Estimating Visual Information From Audio Through Manifold Learning. *arXiv preprint arXiv:2208.02337* (2022). <https://arxiv.org/abs/2208.02337>
- [23] Karol J. Piczak. 2015. ESC: Dataset for Environmental Sound Classification. In *Proceedings of the 23rd Annual ACM Conference on Multimedia (Brisbane, Australia, 2015-10-13)*. ACM Press, 1015–1018. doi:10.1145/2733373.2806390
- [24] Can Qin, Ning Yu, Chen Xing, Shu Zhang, Zeyuan Chen, Stefano Ermon, Yun Fu, Caiming Xiong, and Ran Xu. 2023. GlueGen: Plug and Play Multi-modal Encoders for X-to-image Generation. In *Proceedings of the IEEE/CVF International Conference on Computer Vision (ICCV)*. 23085–23096.
- [25] Alec Radford, Jong Wook Kim, Chris Hallacy, Aditya Ramesh, Gabriel Goh, Sandhini Agarwal, Girish Sastry, Amanda Askell, Pamela Mishkin, Jack Clark, et al. 2021. Learning transferable visual models from natural language supervision. In *International conference on machine learning*. PmlR, 8748–8763.
- [26] Colin Raffel, Noam Shazeer, Adam Roberts, Katherine Lee, Sharan Narang, Michael Matena, Yanqi Zhou, Wei Li, and Peter J. Liu. 2020. Exploring the Limits of Transfer Learning with a Unified Text-to-Text Transformer. *Journal of Machine Learning Research* 21, 140 (2020), 1–67. <http://jmlr.org/papers/v21/20-074.html>
- [27] Aditya Ramesh, Prafulla Dhariwal, Alex Nichol, Casey Chu, and Mark Chen. 2022. Hierarchical text-conditional image generation with clip latents. *arXiv preprint arXiv:2204.06125* 1, 2 (2022), 3.
- [28] Aditya Ramesh, Mikhail Pavlov, Gabriel Goh, Scott Gray, Chelsea Voss, Alec Radford, Mark Chen, and Ilya Sutskever. 2021. Zero-shot text-to-image generation. In *International conference on machine learning*. Pmlr, 8821–8831.
- [29] Robin Rombach, Andreas Blattmann, Dominik Lorenz, Patrick Esser, and Björn Ommer. 2022. High-resolution image synthesis with latent diffusion models. In *Proceedings of the IEEE/CVF conference on computer vision and pattern recognition*. 10684–10695.
- [30] Vignesh Subramaniam, Colin Conwell, Chen Wang, Gabriel Kreiman, Boris Katz, Ignacio Cases, and Andrei Barbu. 2024. Revealing Vision-Language Integration in the Brain with Multimodal Networks. *arXiv preprint arXiv:2406.14481* (2024). <https://arxiv.org/abs/2406.14481> PMID: 38947929; PMCID: PMC11213144.
- [31] Kim Sung-Bin, Arda Senocak, Hyunwoo Ha, Andrew Owens, and Tae-Hyun Oh. 2023. Sound to Visual Scene Generation by Audio-to-Visual Latent Alignment. *arXiv preprint arXiv:2303.17490* (2023). <https://arxiv.org/abs/2303.17490>
- [32] Zineng Tang, Ziyi Yang, Chenguang Zhu, Michael Zeng, and Mohit Bansal. 2023. Any-to-any generation via composable diffusion. *Advances in Neural Information Processing Systems* 36 (2023), 16083–16099.
- [33] C.-H. Wan, S.-P. Chuang, and H.-Y. Lee. 2019. Towards audio to scene image synthesis using generative adversarial network. In *ICASSP 2019 - IEEE International Conference on Acoustics, Speech and Signal Processing (ICASSP)*. 496–500.
- [34] Jason Wei, Xuezhi Wang, Dale Schuurmans, Maarten Bosma, Fei Xia, Ed Chi, Quoc V Le, Denny Zhou, et al. 2022. Chain-of-thought prompting elicits reasoning in large language models. *Advances in neural information processing systems* 35 (2022), 24824–24837.
- [35] Han Wenjuan, Wei Xiang, Cui Xingyu, Cheng Ning, Jiang Guangyuan, Qian Weinan, and Zhang Chi. 2024. Prompt Engineering 101 Prompt Engineering Guidelines from a Linguistic Perspective. In *Proceedings of the 23rd Chinese National Conference on Computational Linguistics (Volume 1: Main Conference)*, Maosong Sun, Jiye Liang, Xianpei Han, Zhiyuan Liu, and Yulan He (Eds.). Chinese Information Processing Society of China, Taiyuan, China, 1408–1426. <https://aclanthology.org/2024.ccl-1.108/>
- [36] Guy Yariv, Itai Gat, Sagie Benaim, Lior Wolf, Idan Schwartz, and Yossi Adi. 2024. Diverse and aligned audio-to-video generation via text-to-video model adaptation. In *Proceedings of the AAAI Conference on Artificial Intelligence*, Vol. 38. 6639–6647.
- [37] Guy Yariv, Itai Gat, Lior Wolf, Yossi Adi, and Idan Schwartz. 2023. Audio-Token: Adaptation of Text-Conditioned Diffusion Models for Audio-to-Image Generation. In *Interspeech*. 5446–5450.
- [38] Guy Yariv, Itai Gat, Lior Wolf, Yossi Adi, and Idan Schwartz. 2023. AudioToken: Adaptation of Text-Conditioned Diffusion Models for Audio-to-Image Generation. *arXiv preprint arXiv:2305.13050* (2023). <https://arxiv.org/abs/2305.13050>
- [39] Yipin Zhou, Zhaowen Wang, Chen Fang, Trung Bui, and Tamara L. Berg. 2018. Visual to Sound: Generating Natural Sound for Videos in the Wild. In *Proceedings of the IEEE Conference on Computer Vision and Pattern Recognition (CVPR)*.